Generalized Collision-free Velocity Model for Pedestrian Dynamics

Qiancheng Xu[1,2]**, Mohcine Chraibi**[1,2] **and Antoine Tordeux**[3]

[1] *Institute of Advanced Simulation (IAS-7),*
Forschungszentrum Jülich GmbH, 52425 Jülich, Germany

[2] *Department of Computer Simulation for Fire Safety and Pedestrian Traffic,*
University of Wuppertal, 42119 Wuppertal, Germany

[3] *School of Mechanical Engineering and Safety Engineering,*
University of Wuppertal, 42119 Wuppertal, Germany

emails: `q.xu@fz-juelich.de`, `m.chraibi@fz-juelich.de`, `tordeux@uni-wuppertal.de`

Abstract

The collision-free velocity model is a microscopic pedestrian model, which despite its simplicity, reproduces fairly well several self-organisation phenomena in pedestrian dynamics. The model is composed of two components: a direction sub-model which combines individual desired direction and neighbour's influence to imitate the process of navigating in a two-dimensional space, and an intrinsically collision-free speed sub-model which controls the speed of the agents based on the distance to their surroundings.

Although the model performs well is many scenarios, it's minimal character can be improved by further extensions. Firstly, the model definition is shape specific. Circles are used to express the projection of pedestrian's body on the two-dimensional plane, however many references and researches indicate that dynamical ellipses can represent pedestrian's shape more accurately. Secondly, the change of the direction is per definition performed instantaneously in every time step, which leads to an unnatural "shaking" of pedestrians during simulations.

This paper generalises the collision-free velocity model by extending the distance calculations to velocity-based ellipses. Besides, we introduce enhancement to the direction sub-module of the model, which smooths the direction changes of pedestrians in the simulation; a shortcoming that was not visible in the original model due to the symmetry of the circular shapes. Furthermore, we study the effects of the pedestrian's shape on the simulation's result.

We validate our enhancements by comparing the simulation results with the flow through a bottleneck for different widths of the exit. The model is implemented within the open source software JuPedSim.

Key words: Collision-free velocity model, dynamical ellipse, improvement, validation

1 Introduction

Nowadays, the scale of some activities is getting bigger with the increasing of world population and the convenience of transport. Although these events usually are carefully planned before they are held, the probability of accidents still increase as the participant's number increases. Therefore, before planning the event and in order to avoid accidents in advance, simulations based on the situation of the site like the number of participants, the structure of building, can be a major asset [1-3].

In General models used to describe pedestrian dynamics can be categorized as , macroscopic [4-8] and microscopic models. Macroscopic models use average quantities of pedestrian flow, e.g. density, velocity and flow, to describe the overall state of a group of pedestrians, whereas microscopic models consider each pedestrian's movement individually. Compared to macroscopic models, a microscopic model is often more complex, but can represent the behaviour of pedestrians in more details.

After up to 50 years of development, many kinds of microscopic models exist in the literature, which can reproduce fairly well several collective phenomena in pedestrian dynamics. These models include cellular automate models [9-13], force-based models [14-17] and velocity models [18-21]. In this paper we focus on the extension of the collision-free velocity model introduced in [19].

The collision-free velocity model (CVM) is composed of a velocity and a direction submodels. Unlike most force-based models, CVM is per definition collision free. Moreover, the model is based on an ordinary differential equation of first-order, therefore their computational complexity compared to second-order models can be significantly reduced by adopting bigger time steps during simulation. This comes handy when performing large scale simulations is necessary.

CVM has five parameters. It can reproduce a large range of dynamics observed in real pedestrian flows. In this paper, we mainly made two extensions based on this minimal model. Firstly, we change the shape of agents from circle to ellipse. In the original model, circles are used to express the projection of pedestrian's body on the two-dimensional plane, however many references and researches indicate that dynamical ellipse can represent pedestrian's shape more accurately, because the space a pedestrian occupies is influenced by the length of the legs during the motion and the lateral swaying of the body. Therefore, we generalise CVM by extending the distance calculation to velocity-based ellipse and compare the simulation results with the original model (circles). After introducing the first extension, an unnatural "shaking" was observed during the simulation, which is caused by the zero-order direction sub-model. Therefore, we propose a new first-order direction sub-model, designed to smooth the direction changes of pedestrians in the simulation.

For the sake of completeness, we introduce the original CVM in section 2. The generalisation of the model from circle-based to ellipse-based definition and the comparison between simulation results of circle and ellipse is given in section 3. In section 4, a new direction submodel is proposed and the performances are compared to the original CVM. A conclusion is made to summarise these extensions and point out to limitations of the model as well as future

research directions.

2 Collision-free velocity model

We introduce in this section the collision-free velocity model [19]. In the original model, the moving direction and velocity of each pedestrian are updated at each time step. At every update moment, moving direction of a pedestrian is obtained by integrating influence of surrounding pedestrians and the desired direction. Then the value of velocity depends on the minimal spacing in the moving direction obtained before. In order to illustrate the original model clearly, we quote figure 1 (borrowed from [19]). In figure 1, pedestrians are represented by circle with constant diameter ℓ. X_i, X_j and X_k are the two dimensional positions of pedestrian i, j and k. The original CVM can be described as

$$\dot{X}_i(X_i, X_j, \dots) = V_i(X_i, X_j, \dots) * \vec{e}_i(X_i, X_j, \dots), \tag{1}$$

where V_i is the velocity of pedestrian i and $\vec{e}_i$ is the moving direction.
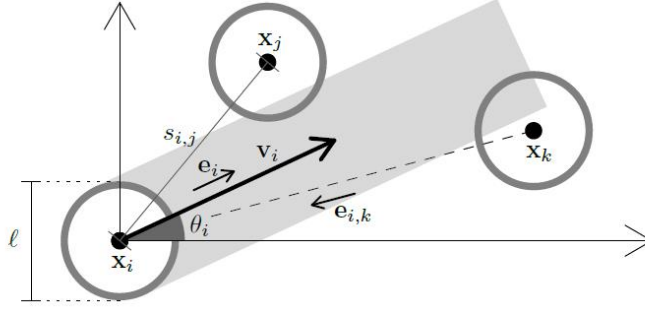

Figure 1: Notations used in collision-free velocity model(borrowed from [19])

Moving direction $\vec{e}_i$ is obtained from the direction sub-model

$$\vec{e}_i(X_i, X_j, ...) = \frac{\vec{e}_i^{\,0} + \sum_{j \in N_i} R(s_{i,j}) \cdot \vec{e}_{i,j}}{||\vec{e}_i^{\,0} + \sum_{j \in N_i} R(s_{i,j}) \cdot \vec{e}_{i,j}||}. \tag{2}$$

where $\vec{e}_i^{\,0}$ is the desired direction given by a strategic model, N_i is the set containing all the neighbours of pedestrian i, $\vec{e}_{i,j}$ is the unit vector from the centre of pedestrian j towards the centre of pedestrian i. The repulsive function

$$R(s_{i,j}) = a \cdot \exp\left(\frac{\ell - s_{i,j}}{D}\right) \tag{3}$$

is used to describe the influence that neighbours act on the moving direction of pedestrian i. As mentioned before, ℓ is the diameter of the circle used to represent the pedestrians and $s_{i,j}$

is the distance between the centres of pedestrian i and j. There are two parameters in the repulsive function, the scale coefficient $a > 0$ and distance coefficient $D > 0$.

After obtaining the moving direction $\vec{e}_i$, the speed model

$$V_i(s_{i,j}) = \min\left\{V_i^0, \max\left\{0, \frac{s_i - \ell}{T}\right\}\right\} \tag{4}$$

is used to determine the scale of velocity V_i in the direction $\vec{e}_i$. In equation (4), V_i^0 is the desired speed of pedestrian i and

$$s_i = \min_{j \in J_i} s_{i,j} \tag{5}$$

is the distance between the centre of pedestrian i and the centre of the closet pedestrian in front of i, when pedestrian i moving in the direction $\vec{e}_i$. The definition of set J_i in equation (5) is

$$J_i = \left\{j, \vec{e}_i \cdot \vec{e}_{i,j} \leq 0 \text{ and } \left|\vec{e}_i^{\perp} \cdot \vec{e}_{i,j}\right| \leq \frac{\ell}{s_{i,j}}\right\}, \tag{6}$$

where $\vec{e}_i^{\perp} \cdot \vec{e}_i = 0$, J_i is the set contains all the pedestrians overlapping with the grey area in figure 1. The only coefficient in the speed model is $T > 0$ which is used to adjust the gap between pedestrians. The gap between pedestrians become smaller with the decreasing of T.

Above is the definition of original collision-free velocity model, how pedestrians influence each other was described specifically but how to deal with the influence of wall is not mentioned in the original model [19]. In order to implement this collision-free velocity model in JuPedSim (a free software developed by IAS-7 in Forschungszentrum Jülich GmbH), we complete the way used to calculate the influence between pedestrians in original model to obtain the influence of walls. In Figure 2, X_i, $\vec{e}_i$ and V_i have the same definitions as in figure 1. Besides, there are two walls in the figure, wall j and k. C_j and C_k are the closest points in wall j and k to the centre of pedestrian i respectively. $\vec{e}_{i,w_j}$ and $\vec{e}_{i,w_k}$ are the unit vectors from C_j and C_k to X_i. s_{i,w_j} and s_{i,w_k} are the distances from C_j and C_j to X_i. The angle between $\vec{e}_i$ and $-\vec{e}_{i,w_j}$ is α_j. While the angle between $\vec{e}_i$ and $-\vec{e}_{i,w_k}$ is α_k.

After introducing the influence of walls, the direction model becomes

$$\vec{e}_i = \frac{\vec{e}_i^{\,0} + \sum_{j \in N_i} R(s_{i,j}) \cdot \vec{e}_{i,j} + \sum_{j \in W_i} R_w(s_{i,w_j}) \cdot \vec{e}_{i,w_j}}{||\vec{e}_i^{\,0} + \sum_{j \in N_i} R(s_{i,j}) \cdot \vec{e}_{i,j} + \sum_{j \in W_i} R_w(s_{i,w_j}) \cdot \vec{e}_{i,w_j}||}, \tag{7}$$

where W_i is the set contains all the walls nearby pedestrian i, and

$$R_w(s_{i,w_j}) = a_w \cdot \exp\left(\frac{\frac{\ell}{2} - s_{i,w_j}}{D_w}\right). \tag{8}$$

In order to avoid pedestrians cross walls directly, walls should not only influence pedestrian's moving direction, but also the scale of the velocity. The expanded speed model is

$$V_i = \min\left\{V_i^0, \max\left\{0, \frac{s_i - \ell}{T}\right\}, \max\left\{0, \frac{sw_i}{T}\right\}\right\}, \tag{9}$$
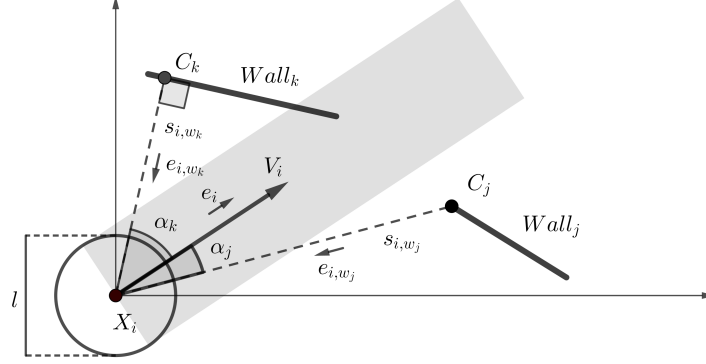
Figure 2: Notations used in collision-free velocity model when calculating the influence of walls on the direction and scale of pedestrian's velocity.

where the definitions of s_i, ℓ, T are same as in equation (4) and

$$sw_i = \min_{j \in JW_i} \frac{s_{i,w_j} - \frac{\ell}{2}}{\cos \alpha_j}, \tag{10}$$

where JW_i is the set containing all the walls in the moving direction of pedestrian i (grey area in figure 2). The original model becomes complete and can be implemented in JuPedSim after introducing the influence of walls.

3   From circle to ellipse

We generalize the collision-free velocity model by extending the distance calculations to velocity-based ellipses in this section. We define the ellipse with major semiaxis a and minor semiaxis b to represent the shape of pedestrian i on the two-dimensional plane. In the following, a is the required space in the move direction $\vec{e}_i$. We set

$$a = a_{min} + \tau_a V_i, \tag{11}$$

where V_i is the velocity of pedestrian i, while $a_{min} > 0$ and $\tau_a > 0$ are two parameters. b is the semi-width of pedestrian i in orthogonal direction of $\vec{e}_i$. We set

$$b = b_{max} - (b_{max} - b_{min}) \frac{V_i}{V_i^0}, \tag{12}$$

with b_{min} is the minimum semi-width when the velocity of pedestrian i reach his desired velocity V_i^0 and b_{max} is the maximum semi-width when pedestrian i is static (see figure 3).

The definition of symbols in figure 3 are already introduced in figure 1 and figure 2. There are two pedestrians and one wall in figure 3. The ellipse in full line describes the pedestrian
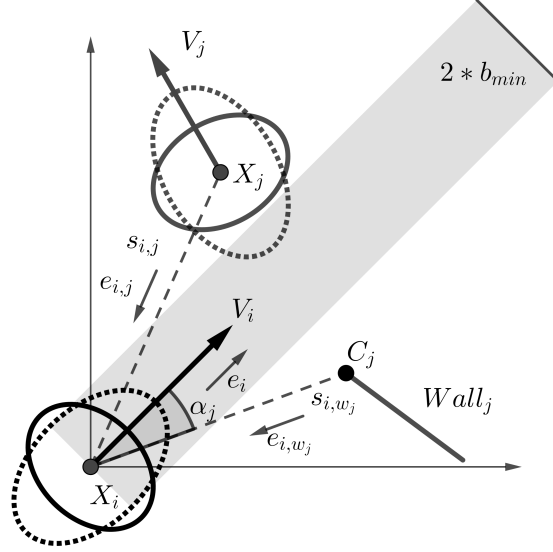
Figure 3: Notations used in the collision-free velocity model after extending the distance calculations between pedestrians from circle to velocity-based ellipses

when static, while the ellipse in dashed line represents the pedestrian at desired velocity. Since the shape of ellipse is time-varying, the calculation about ellipses become much more complex compared to circles.

The basic structure of the model stays the same, moving direction $\vec{e}_i$ is calculated firstly via equation (7), where

$$R(s_{i,j}) = a \cdot \exp\left(\frac{d_{i,j}}{D}\right), \tag{13}$$

$$R_w(s_{i,w_j}) = a_w \cdot \exp\left(\frac{d_{i,w_j}}{D_w}\right) \tag{14}$$

are changed. $d_{i,j}$ is the distance between the borders of the ellipses, along a line connecting X_i and X_j. d_{i,w_j} is the distance between the wall j and the border of ellipse used to present pedestrian i, along a line connecting X_i and C_j. We have to notice that $d_{i,j}$ and d_{i,j_w} can be nonzero even when pedestrian i overlap or touch with other pedestrians or walls.

Then the velocity V_i is obtained by using

$$V_i = \min\left\{V_i^0, \max\left\{0, \frac{s_i - b_i - b_j}{T}\right\}, \max\left\{0, \frac{sw_i}{T}\right\}\right\}, \tag{15}$$

where the definition of s_i is given in equation (5) and

$$sw_i = \min_{j \in JW_i} \frac{s_{i,w_j} - b_i}{\cos \alpha_j}. \tag{16}$$

Here J_i and JW_i are sets containing all pedestrians and walls in front (i.e. the grey area in figure 3). b_i and b_j are the semi-width of ellipses used to present pedestrians i and j, respectively.

we reduce $b_i + b_j$ when calculating the distance between two ellipses, and reduce b_i when calculating the distance between ellipse and wall, because it's a very complex and expensive process to calculate the closet distance between two ellipses, moreover ellipses are more easy to locked by each other compared to circles. In order to keep the property of collision-free, we see pedestrian a dynamical circle with radius b when getting the velocity.

Another difference between circle and ellipse is the width of the grey area is ℓ in circle case while it is $2 * b_{min}$ in case of ellipse. The purpose of using $2 * b_{min}$ instead of the dynamic width of ellipse is to avoid some unrealistic blocking in simulation. Pedestrians should accelerate to cross gaps smaller than the dynamic width of ellipse but bigger than $2 * b_{min}$. Although a very small overlap between ellipses appear sometimes when the width of grey area is set as $2 * b_{min}$, the degree of overlap is acceptable and can eliminate some undesired blocking and make the model more realistic.

After transfer from circle to ellipse, we validate the model by using the experimental data from the bottleneck scenario. We measure the relation between the flow in the middle of the bottleneck with the width of bottleneck, the width of bottleneck is from 1.0 m to 2.5 m. Then adjust the parameters of model to make the relation obtained from the simulation result as close to the relation from experimental data as possible. The validation result is shown in figure 4 we can find the simulation result of circle and ellipse both very close to the experimental data.
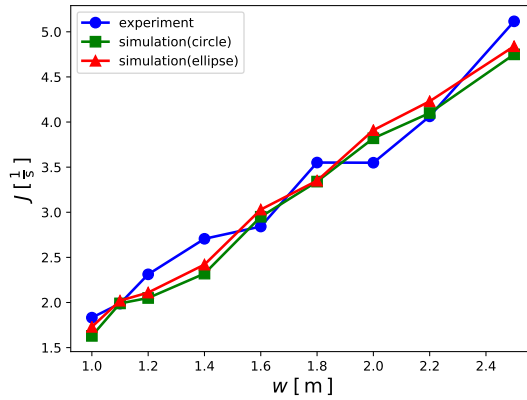

Figure 4: Validation result of collision-free velocity model using circle and dynamical ellipse to represent the shape of pedestrians respectively, experimental data obtained in the DFG-project

The desire velocity of pedestrians are Gaussian distributed with mean 1.34 m/s and standard deviation 0.26 m/s. The values of the other parameters are shown in table 1. Since the model is collision-free, the size of agent is a little smaller than in force-based model.

After validation, we measure the fundamental diagram in the two-dimensional space for

Table 1: parameters of the collision-free velocity models using circle and dynamical ellipse to represent the shape of pedestrians respectively

Shape	V^0 (m/s)	b_{min} (m)	b_{max} (m)	a_{min} (m)	τ_a (s)	a	D (m)	a_w	D_w (m)	T (s)
Ellipse	(1.34, 0.26)	0.15	0.20	0.13	0.1	3.0	0.1	6.0	0.05	0.55
Circle	(1.34, 0.26)	0.18	0.18	0.18	0	3.0	0.1	6.0	0.05	0.5

circular and elliptic shapes of pedestrian, respectively. The simulation scenario is a 26×1.8 m² corridor with periodic boundary conditions. The simulation results are compared to experimental data. The parameters used in the simulation are same as the parameters in table 1.
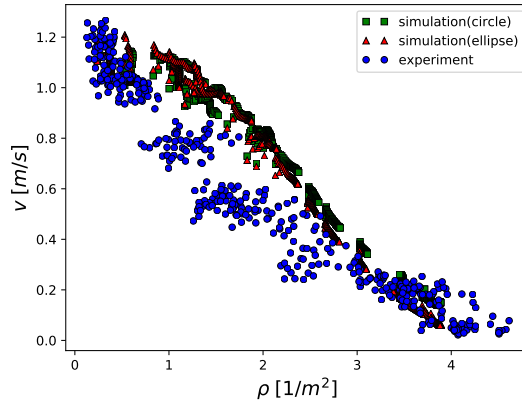

Figure 5: Density-velocity relation of collision-free velocity model using circle and dynamical ellipse to represent the shape of pedestrians respectively, in a 26×1.8 m² corridor, compared with experimental data obtained in the HERMES-project.

From figure 5, we can find that when the density is small, the velocity obtained from simulation both higher than the velocity obtained from experiment data. When the density become bigger, the simulation result approaches experiment result, and the simulation result for ellipse is much closer to the experiment data. We have to mentioned here that we can adjust the parameters to obtain a better fundamental diagram which much closer to the experimental data, but it results in the deviation between the simulation result and experiment in bottleneck scenario. we think the reason is that pedestrian need more cooperation in bottleneck to increase the flow than in a corridor. This will be our future research area.

4 New direction sub-model

After transferring from circle to ellipse, we found some impractical behaviour during simulation in bottleneck scenario. First of all, backward movements occur too often, which is not realistic especially in evacuation scenarios. Secondly, an unnatural "shaking" appear during simulation, which was not visible when the shape of pedestrian is circle due to the symmetry of the circular shapes.

In order to disappear these two unrealistic behaviour, we introduce enhancement to the direction sub-module. In original model, moving direction $\vec{e}_i$ of pedestrian i is calculated by combining individual desire direction $\vec{e}_i^{\,0}$ and neighbours (pedestrians and walls) influence. Since the direction of neighbours influence is from the centre of pedestrian or closest point on wall towards the centre of pedestrian i, the influence can be divided into two part, one perpendicular to $\vec{e}_i^{\,0}$ and the other one is parallel to $\vec{e}_i^{\,0}$. The parallel part is the reason of backward movements. Actually, pedestrian hardly choose a moving direction whose parallel part of $\vec{e}_i^{\,0}$ is in the inverse direction of $\vec{e}_i^{\,0}$. Based on this idea, we propose a new direction sub-module as shown in figure 6. In figure 6, $\vec{e}_i^{\,0}$ is the desired direction of pedestrian i. $\vec{e}_i^{\,0\perp}$ and $\vec{e}_i^{\perp}$ are the normalized left side perpendicular vector of $\vec{e}_i^{\,0}$ and $\vec{e}_i$ respectively.
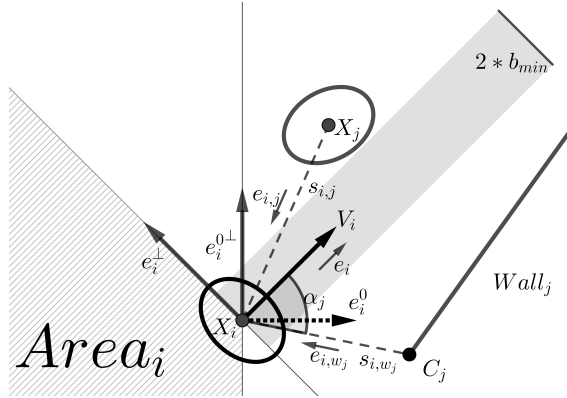

Figure 6: Notations used in collision-free velocity model calculating direction of velocity via new direction sub-model

In the new direction sub-module, we use

$$\vec{e}_i = \frac{\vec{e}_i^{\,0} + \sum_{j \in N_i} R(s_{i,j}) \cdot \vec{e}_{i,j}^{\,N} + \sum_{j \in W_i} R_w(s_{i,w_j}) \cdot \vec{e}_{i,w_j}^{\,N}}{||\vec{e}_i^{\,0} + \sum_{j \in N_i} R(s_{i,j}) \cdot \vec{e}_{i,j}^{\,N} + \sum_{j \in W_i} R_w(s_{i,w_j}) \cdot \vec{e}_{i,w_j}^{\,N}||}, \tag{17}$$

to calculate $\vec{e}_i$. The repulsive function $R(s_{i,j})$ and $R_w(s_{i,w_j})$ are still given by equation (13) and equation (14) and

$$\vec{e}_{i,j}^{\,N} = \begin{cases} \vec{e}_i^{\,0\perp}, (\vec{e}_i^{\,0} \times \vec{e}_{i,j}) * (\vec{e}_i^{\,0} \times \vec{e}_i^{\,0\perp}) \geq 0 \\ -\vec{e}_i^{\,0\perp}, (\vec{e}_i^{\,0} \times \vec{e}_{i,j}) * (\vec{e}_i^{\,0} \times \vec{e}_i^{\,0\perp}) < 0 \end{cases} \tag{18}$$

$$\vec{e}_{i,w_j}^{N} = \begin{cases} \vec{e}_i^{0\perp}, (\vec{e}_i^{0} \times \vec{e}_{i,w_j}) * (\vec{e}_i^{0} \times \vec{e}_i^{0\perp}) \geq 0 \\ -\vec{e}_i^{0\perp}, (\vec{e}_i^{0} \times \vec{e}_{i,w_j}) * (\vec{e}_i^{0} \times \vec{e}_i^{0\perp}) < 0 \end{cases} \qquad (19)$$

According to equation (18) and equation (19), influence directions of pedestrians and walls are decided not only by their position but also by the desired direction of pedestrian i. If the centre of pedestrians or the closest point of walls are located in the left side of $\vec{e}_i^{0}$, influence direction is right side perpendicular vector of $\vec{e}_i^{0}$ and vice versa. It should be noticed that there is a special case when $\vec{e}_i^{0} \times \vec{e}_{i,j}$ or $\vec{e}_i^{0} \times \vec{e}_{i,w_j}$ are equal to zero. In this case, the influence direction is decided by multiple factors, e.g. culture, gender. In order to simplify the model, we set the influence direction is always left side perpendicular vector of $\vec{e}_i^{0}$ in this case.

Besides the influence direction, we proposed a dynamical vision area, which is the white area in figure 6. Pedestrians and walls located in $Area_i$, which is the hatching area in figure 6, do not influence the moving direction of pedestrian i. The set contains all neighbours of pedestrian i in $Area_i$ is

$$N_i^{Area} = \left\{ j, \vec{e}_i \cdot \vec{e}_{i,j} < 0 \text{ and } \vec{e}_i^{0} \cdot \vec{e}_{i,j} < 0 \right\}. \qquad (20)$$

Only when both of two vertices of walls are in $Area_i$, walls do not influence the moving direction of pedestrian i. Vision area of pedestrian i is decided by his desire moving direction $\vec{e}_i^{0}$ and his actual moving direction $\vec{e}_i$. This means a pedestrian choose the best moving direction not only according to the pedestrians and walls in front of his moving direction, but also in front of his desire moving direction. Using this dynamical vision area can eliminate some unrealistic block occurred between agents when using fixed vision area in the simulation.

These two enhancements can eliminate the phenomena of backward movement in the simulation. However the unnatural "shaking" still exist. The cause of the "shaking" is that pedestrian turn to $\vec{e}_i$ directly after calculation in original model (0th order model), so our solution is introducing a smooth process (e.g. a relaxation process). We change the direction sub-module from zero-order to first-order, which does not change the global first-order property of the original CVM. We introduce a new relaxation time parameter τ in the original direction sub-model, the new direction sub-module is represented in discrete time as

$$\vec{e}_i^{new}(t) = \begin{cases} \vec{e}_i^{new}(t - \Delta t) + \frac{\vec{e}_i(t) - \vec{e}_i^{new}(t - \Delta t)}{\tau} * \Delta t, \ \vec{e}_i(t) \cdot \vec{e}_i^{new}(t - \Delta t) > 0 \\ \vec{e}_i(t), \ \vec{e}_i(t) \cdot \vec{e}_i^{new}(t - \Delta t) \leq 0 \end{cases} , \qquad (21)$$

where $\vec{e}_i^{new}$ is the moving direction of pedestrian i calculated by new direction sub-module and $\vec{e}_i$ is calculated by equation (7). By adjusting τ, pedestrian can turn to moving direction smoothly. It should be noticed that after introducing the first extension about influence direction, we can eliminate almost all the oscillation in the simulation excepted when the desired direction $\vec{e}_i^{0}$ changes a lot suddenly. In this case, $\vec{e}_i(t) \cdot \vec{e}_i^{new}(t - \Delta t) > 0$ may not be met, pedestrians turn to $\vec{e}_i$ directly. This is consistent with the reality, pedestrians change their moving direction directly if they change desire direction from one exit to another exit.

We validate the new model by the same way as previously. The validation results are compared to experiment data and the original model in figure 7. The shape of pedestrian in original model and new model are both ellipse here, the parameters are shown in table 2.
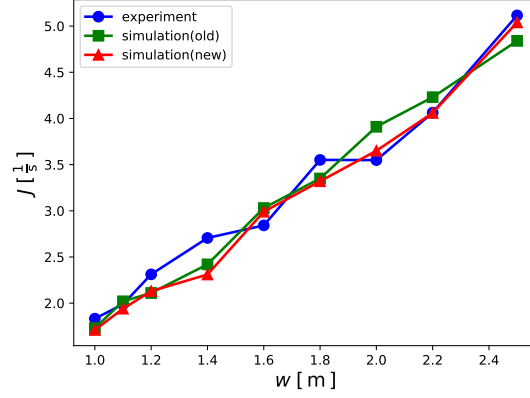
Figure 7: Validation result of collision-free velocity model calculating moving direction via original direction sub-model and new ones respectively, experimental data obtained in the DFG-project

Table 2: parameters of the collision-free velocity models calculating moving direction via original direction sub-model and new ones respectively

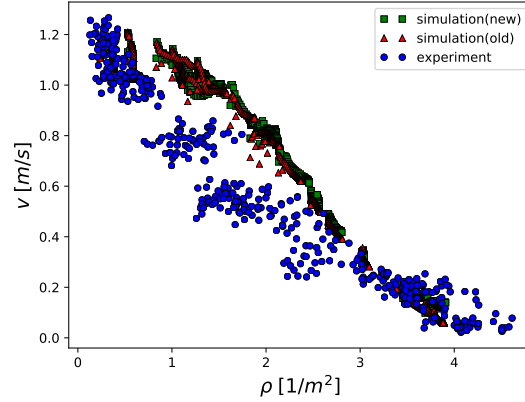| Model	V^0 (m/s)	b_{min} (m)	b_{max} (m)	a_{min} (m)	τ_a (s)	a	D (m)	a_w	D_w (m)	T (s)	τ (s)
Original	(1.34, 0.26)	0.15	0.20	0.13	0.1	3.0	0.1	6.0	0.05	0.55	\
New	(1.34, 0.26)	0.15	0.20	0.13	0.1	3.0	0.1	6.0	0.05	0.55	0.3

Figure 8: Density-velocity relation of collision-free velocity model calculating moving direction via original direction sub-model and new ones respectively, in a 26×1.8 m^2 corridor, compared with experimental data obtained in the HERMES-project.

11

After obtain the parameters, we compare the fundamental diagram of the original model and the new model. The result is shown in figure 8. From figure 8 we can find that our extensions do not change significantly the fundamental diagram of the original model.

Since the purpose of our extension is to eliminate backward movement and shaking phenomenon. We compare two index here to prove that our extensions are useful. The first one is average oscillation times, which can be calculated by

$$O_{average} = \frac{\sum\limits_{k=0}^{k=M} \sum\limits_{i=1}^{i=N} O_i(k * \Delta t)}{N}, \tag{22}$$

where $M * \Delta t$ is the simulation duration, Δt is the time step, N is the number of pedestrians in the simulation and

$$O_i(t) = \begin{cases} 1, & \vec{e}_i(t) \cdot \vec{e}_i^{\,0}(t) < 0 \\ 0, & else \end{cases}. \tag{23}$$

in the original model and

$$O_i(t) = \begin{cases} 1, & \vec{e}_i^{\,new}(t) \cdot \vec{e}_i^{\,0}(t) < 0 \\ 0, & else \end{cases}. \tag{24}$$
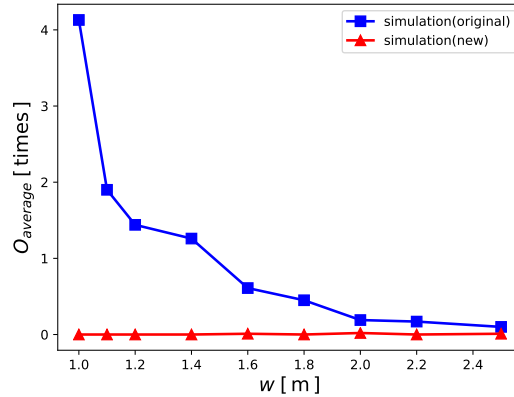
in the new model.

Figure 9: Average oscillation times of each agents in the collision-free velocity models calculating moving direction via original direction sub-model and new ones respectively, scenarios of simulation are the bottlenecks with width from 1.0 m to 2.5 m, the number of agents involved in the simulation is 50.

When the degree between the moving direction and desire direction of a pedestrian is larger than 90 degree, we see it as an oscillation. We compare the oscillation index of the new model to the original model in figure 9. From figure 9, we can find that the average oscillation

times significantly decrease in the new model compared to the original model. Therefore our extension eliminate the unrealistic oscillation movement.

The second index is average shaking index, which is presented as

$$S_{average} = \frac{\sum\limits_{k=1}^{k=M} \sum\limits_{i=1}^{i=N} S_i(k * \Delta t)}{N}, \tag{25}$$

with

$$S_i(t) = \left| \angle \vec{e}_i(t) - \angle \vec{e}_i(t - \Delta t) \right|. \tag{26}$$

in the original model and

$$S_i(t) = \left| \angle \vec{e}_i^{\,new}(t) - \angle \vec{e}_i^{\,new}(t - \Delta t) \right|. \tag{27}$$

in the new model. $S_i(t)$ is the absolute difference between the angles of moving direction in the current time step and the previous one. We compare the average shaking index of the new model and the original model, the result is shown in figure 10.
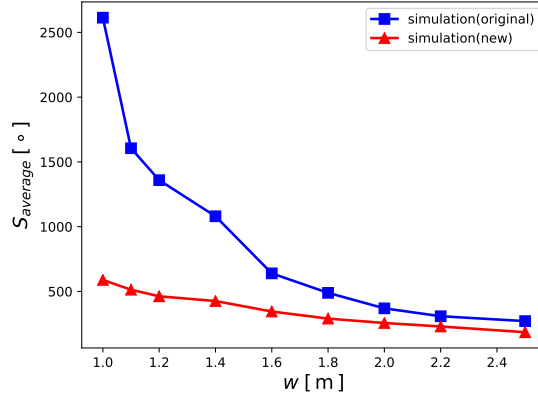

Figure 10: Average shaking degree of collision-free velocity model calculating moving direction via original direction sub-model and new ones respectively,scenarios of simulation are the bottlenecks with width from 1.0 m to 2.5 m, the number of agents involved in the simulation is 50.

It can be observed in figure 10 that in the new model the pedestrians change less their direction than the pedestrians in original model, which is in line with the fact that pedestrian prefer to keep their direction instead of change it.

5   Conclusion

In this paper we complete the collision-free velocity model by introduce the influence of walls. Then, we generalise the model by using dynamical ellipse instead of circle to represent the

projection of pedestrians in the two-dimensional plane. Although the performances with ellipses are not significantly better than with circles, we find that some unrealistic phenomena occurred in the simulation, which are caused by the direction sub-model. In order to eliminate these unrealistic behaviours of the pedestrians, a new direction sub-model is proposed. Simulation results show that the new direction sub-model can remove these behaviours without breaking the advantages of original model.

Although the extended model proposed in this paper performs pretty good, there are still many problems that have not been solved yet. First of all, jamming arch appear in the scenario of bottleneck with small width. Secondly, the new model performs not as good as the original model in scenarios of bidirectional flows, because the pedestrian in the new model can't move backward. These problems will be the topic of future researches.

References

[1] SEYFRIED A, PASSON O, STEFFEN B, et al., *New insights into pedestrian flow through bottlenecks*, Transportation Science, **43(3)** (2009) 395-406.

[2] SCHADSCHNEIDER A, KLINGSCH W, KLPFEL H, et al., *Evacuation dynamics: Empirical results, modeling and applications*, Encyclopedia of complexity and systems science. Springer, New York, NY, (2009) 3142-3176.

[3] DUIVES D C, DAAMEN W, HOOGENDOORN S P., *State-of-the-art crowd motion simulation models*, Transportation research part C: emerging technologies, **37** (2013) 193-209.

[4] BELLOMO N, PICCOLI B, TOSIN A., *Modeling crowd dynamics from a complex system viewpoint*, Mathematical models and methods in applied sciences, **22 Suppl 2** (2012) 1230004.

[5] HELBING D., *A fluid-dynamic model for the movement of pedestrians*, Complex Systems **6** (1992) 391-415.

[6] HUGHES R L., *A continuum theory for the flow of pedestrians*, Transportation Research Part B **36** (2002) 507-535.

[7] HUGHES R L., *The flow of large crowds of pedestrians*, Mathematics and Computers in Simulation **53** (2000) 367-370.

[8] HUGHES R L., *The flow of human crowds*, Annual Review of Fluid Mechanics **35** (2003) 169-182.

[9] BLUE V J, ADLER J L., *Cellular automata microsimulation for modeling bi-directional pedestrian walkways*, Transportation Research Part B: Methodological **35(3)** (2001) 293-312.

[10] BURSTEDDE C, KLAUCK K, SCHADSCHNEIDER A, et al., *Simulation of pedestrian dynamics using a two-dimensional cellular automaton*, Physica A **295(3-4)** (2001) 507-525.

[11] FUKUI M, ISHIBASHI Y., *Self-organized phase transitions in cellular automaton models for pedestrians*, Journal of the physical society of Japan **68(8)** (1999) 2861-2863.

[12] KIRCHNER A, SCHADSCHNEIDER A., *Simulation of evacuation processes using a bionics-inspired cellular automaton model for pedestrian dynamics*, Physica A: statistical mechanics and its applications **312(1-2)** (2002) 260-276.

[13] MURAMATSU M, IRIE T, NAGATANI T., *Jamming transition in pedestrian counter flow*, Physica A: statistical mechanics and its applications **267(3-4)** (1999) 487-498.

[14] HELBING D, MOLNAR P., *Social force model for pedestrian dynamics*, Physical review E, **51(5)** (1995) 4282.

[15] CHRAIBI M, SEYFRIED A, SCHADSCHNEIDER A., *Generalized centrifugal-force model for pedestrian dynamics*, Physical Review E, **82(4)** (2010) 046111.

[16] PARISI D R, GILMAN M, MOLDOVAN H. , *A modification of the social force model can reproduce experimental data of pedestrian flows in normal conditions*, Physica A: Statistical Mechanics and its Applications **388(17)** (2009) 3600-3608.

[17] JOHANSSON A, HELBING D, SHUKLA P K., *Specification of the social force pedestrian model by evolutionary adjustment to video tracking data*, Advances in complex systems, **10(supp02)** (2007) 271-288.

[18] TORDEUX A, SEYFRIED A., *Collision-free nonuniform dynamics within continuous optimal velocity models*, Physical Review E, **90(4)** (2014) 042812.

[19] TORDEUX A, CHRAIBI M, SEYFRIED A., *Collision-free speed model for pedestrian dynamics*, Traffic and Granular Flow'15 (2016) 225-232.

[20] MAURY B, VENEL J., *A discrete contact model for crowd motion*, ESAIM: Mathematical Modelling and Numerical Analysis **45(1)** (2011) 145-168.

[21] PARIS S, PETTR J, DONIKIAN S., *Pedestrian reactive navigation for crowd simulation: a predictive approach*, Computer Graphics Forum. Oxford, UK: Blackwell Publishing Ltd **26(3)** (2007) 665-674.